Journal of Alloys and Compounds 509 (2011) 4632–4635

Contents lists available at ScienceDirect

Journal of Alloys and Compounds

journal homepage: www.elsevier.com/locate/jallcom

Solvothermal synthesis of $Hg_{1-x}Cd_xTe$ nanostructures—Their structural and optical properties

Jayakrishna Khatei*, Naresh Babu Pendyala, K.S.R.K. Rao

Department of Physics, Indian Institute of Science, Bangalore 560012, India

ARTICLE INFO

Article history:
Received 2 July 2010
Received in revised form 7 January 2011
Accepted 19 January 2011
Available online 1 February 2011

Keywords:
Semiconductors
Chemical synthesis
X-ray diffraction
Luminescence
Optical properties

ABSTRACT

This article describes a facile, low-cost, solution-phase approach to the large-scale preparation of $Hg_{1-x}Cd_xTe$ nanostructures of different shapes such as nanorods, quantum dots, hexagonal cubes of different sizes and different compositions at a growth temperature of 180 °C using an air stable Te source by solvothermal technique. The XRD spectrum shows that the crystals are cubic in their basic structure and reveals the variation in lattice constant as a function of composition. The size and morphology of the products were examined by scanning electron microscopy (SEM) and transmission electron microscopy (TEM). The formation of irregular shaped particles and few nano-rods in the present synthesis is attributed to the cetyl trimethylammonium bromide (CTAB). The room temperature FTIR absorption and PL studies for a compositon of $x = 0.8$ gives a band gap of 1.1 eV and a broad emission in NIR region (0.5–0.9 eV) with all bands attributed to surface defects.

1. Introduction

The $Hg_{1-x}Cd_xTe$ (MCT) is one of the most important infrared materials, which is subjected to intensive studies. In the last two decades people have grown MCT by various techniques, among them LPE and MBE are relatively mature technologies dominating the MCT industry due to their flexibility in controlling composition, permitting growth of pn junctions operating at relatively low temperature [1]. However, these techniques are ordinarily costly and complex in fabricating materials [2]. Recently there are few reports on the growth of MCT by colloidal synthesis [3,4]. Its optical properties are widely used for the fabrication of high performance photoconductive and photovoltaic detectors. A major concerns for HgCdTe are impurities that affect the device performance by reducing the minority carrier lifetime. The impurity states in MCT have strong impact on the optical and electrical properties of the material used for device purpose [5–8]. Most of the studies on impurities focus on the observation of luminescence emissions associated with the impurity levels.

In the present study, we have synthesized NIR emitting $Hg_{1-x}Cd_xTe$ nanostructures with different compositions ($x = 0.1$–0.8) by solvothermal method, which is a facile, cost effective and solution growth approach to the large-scale preparation of MCT at relatively low temperature (180 °C) using an air stable and water soluble Te source.

2. Experimental

In a typical procedure for the synthesis of MCT nanocrystals, $Cd(CH_3COO)_2$ (0.1–0.8 mmol), $Hg(CH_3COO)_2$ (0.2–0.9 mmol) and 1 mmol of Na_2TeO_3 were put into a 30 ml stainless steel autoclave with a Teflon liner, then the autoclave was filled with ethylenediamine up to 80% of its volume. Then a reducing reagent $N_2H_4{\cdot}H_2O$ (Hydrazine hydrate) was added. The autoclave was maintained at a constant temperature of 180 °C in a laboratory hot air oven for 24 h. For synthesis of MCT nanorods, the autoclave (50 ml capacity) was filled with a solution of 30 ml of deionized water with 0.1 g of CTAB (cetyl trimethylammonium bromide) instead of ethylenediamine along with 4 ml of ammonia solution and 3 ml of hydrazine hydrate. The nanorods were synthesized at 180 °C for 10 h in hot air oven. The oven was switched off and it was cooled to room temperature naturally. The black precipitate was collected and washed with absolute ethanol and distilled water and then centrifuged in sequence to remove the possible impurities. The final product was dried at 60 °C for 4 h. Films for characterization were made by mixing the powder with PVA (polyvinyl alcohol) solution. PVA solution acts like a matrix during the film formation to hold the powdered nanocrystals while transferring them on to a glass slide. The films were dried at room temperature. Structure, morphology, and elemental composition of the samples were studied using X-ray diffraction (XRD), scanning electron microscopy (SEM), transmission electron microscopy (TEM) and energy dispersive X-ray spectroscopy (EDS) techniques. Low temperature and room temperature photoluminescence (PL) measurements were carried out by TRIAX 550 monochromator based PL system with liquid nitrogen cooled InGaAs detector. Samples were mounted on cold finger of a Janis continuous flow helium cryostat. Argon$^+$ laser with emission wavelength tuned to 514.5 nm is used as excitation source. Absorption/transmission measurements were carried out using Bruker IFS 66v/s Fourier Transform Optical Absorption Spectrometer.

3. Results and discussions

The XRD spectrum in Fig. 1a shows the crystalline structure and phase purity of the as synthesized MCT in ethylenediamine. The

* Corresponding author. Fax: +91 80 2360 2602.
E-mail address: khatei@physics.iisc.ernet.in (J. Khatei).

0925-8388/$ – see front matter © 2011 Elsevier B.V. All rights reserved.
doi:10.1016/j.jallcom.2011.01.134

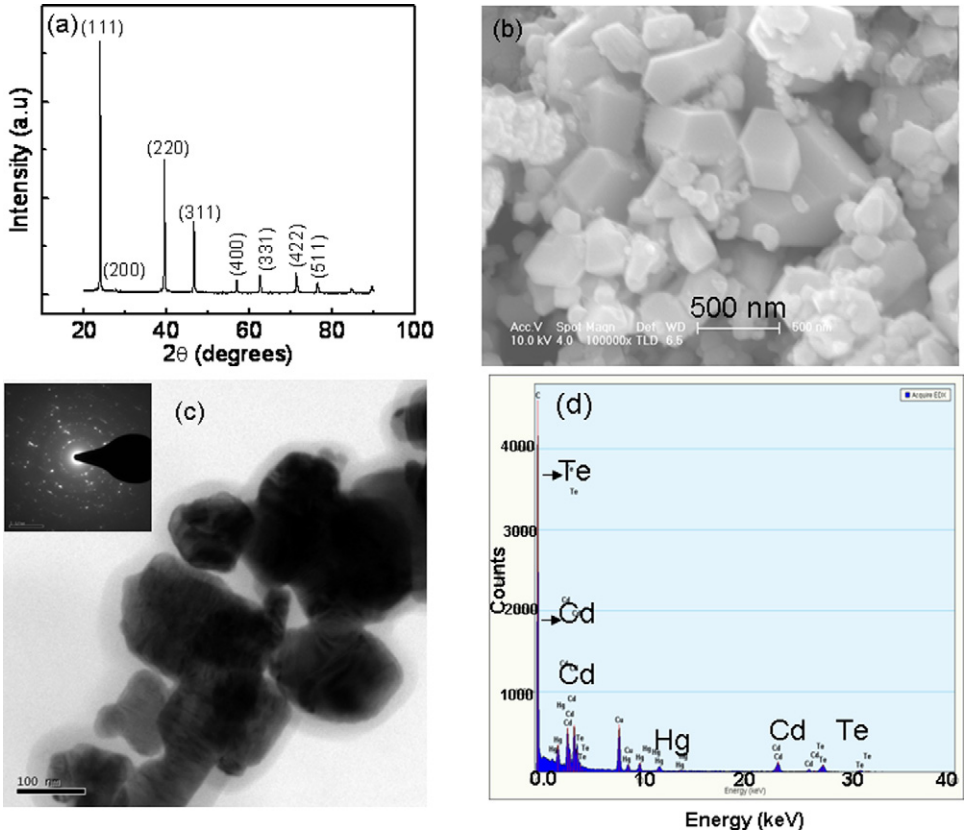

Fig. 1. (A) XRD pattern of $Hg_{1-x}Cd_xTe$ ($x \sim 0.8$) mixed nano- and micro-crystals synthesized in ethylenediamine. (B) FESEM image of $Hg_{1-x}Cd_xTe$ ($x \sim 0.8$) mixed nano- and micro-crystals synthesized in ethylenediamine. (C) TEM micrographs of $Hg_{1-x}Cd_xTe$ ($x \sim 0.8$) mixed nano- and micro-crystals synthesized in ethylenediamine (inset is SAED pattern). (D) EDS spectra of $Hg_{1-x}Cd_xTe$ ($x \sim 0.8$) mixed nano- and micro-crystals synthesized in ethylenediamine, which shows it contains Cd, Hg and Te.

positions of all diffraction peaks match well with a pure $Hg_{1-x}Cd_xTe$ with cubic structure according to the standard card ($a = 6.4654$ Å, JCPDS #51-1122) and that no characteristic peaks from other crystalline forms are present in the XRD pattern. The lattice constants of cubic CdTe and Cubic HgTe according to JCPDS-2000 are respectively 6.49 Å and 6.453 Å. Hence the lattice constant difference between CdTe and HgTe is approximately 0.57%. In the literature there are different values assigned to these lattice constants. As per the reference [9] the lattice constants assigned to the above binary compounds are 6.481 Å, and 6.4603 Å respectively. In this case, the expected lattice mismatch is around 0.32%. The present XRD data (Table 1) closely matches with the reference [9]. In the case of ternary and quaternary compounds, a linear extrapolation of binary compounds, also called Vegard's law [a ($A_{1-x}B_xC$) alloy $= (1-x)a_{AC} + (x)a_{BC}$] is used to find lattice constant, band gap, etc. [10]. However, the lattice constant of bulk $Hg_{1-x}Cd_xTe$ has been measured using XRD by Woolley and Ray in the composition range ($0 \leq x < 1$) with very small deviation from the Vegard's line [11]. Skauli and Colin also measured more accurately the lattice constant ($a = 6.46152 + x^*0.01998$) Å of epitaxially grown $Hg_{1-x}Cd_xTe$ ($0 \leq x < 0.5$) using high resolution XRD [12]. Our experimental data for different compositions though is consistent with the reference [9], also in close agreement with the reference [12].

The TEM micrograph with SAED pattern (Fig. 1c) of MCT confirmed the polycrystalline nature of the sample. The SEM micrographs of MCT sample (Fig. 1b) synthesized in ethylenediamine (en) revealed the hexagonal shape morphology with few random shaped particles, having sizes vary between 20 and 500 nm. This is because in the solvothermal method the shape and size of the nanoparticles depends on the solvent used, reaction temperature and time [13]. The reaction temperature and the solvent play a crucial role in controlling the nucleation and growth of crystallites. Ethylenediamine has the ability to create various shapes due to its high coordinating nature towards the metal cation [14]. Also solvothermal process is a bottom up approach for the formation of nanostructures. A longer synthesis duration will result in bigger particle sizes. In our case we have synthesized for 24 h as a result we got big crystals of 500 nm size. The reaction first involves the dissociation of $Cd(CH_3COO)_2$ and $Hg(CH_3COO)_2$ into Cd^{2+} and Hg^{2+} via their corresponding metal ion complexes $[Cd(en)_2]^{2+}$ and $[Hg(en)_2]^{2+}$ respectively. Secondly, Na_2TeO_3 is reduced to Te^{2-} by $N_2H_4{\cdot}H_2O$ (Hydrazine hydrate). Finally, the Te^{2-} ions reacts with

Table 1
Lattice constants of $Hg_{1-x}Cd_xTe$.

x	(1 1 1)	Lattice constants calculated (Å) from		Lattice constants present data
(Cd)	Peak position (degrees)	Ref.. [9]	Ref. [12]	XRD (Å)
0.1	23.822	6.4624	6.4635	6.4619
0.3	23.808	6.4655	6.4675	6.4656
0.4	23.798	6.4686	6.4731	6.4683
0.5	23.789	6.4707	6.4715	6.4707
0.8	23.765	6.4769	6.4775	6.4771

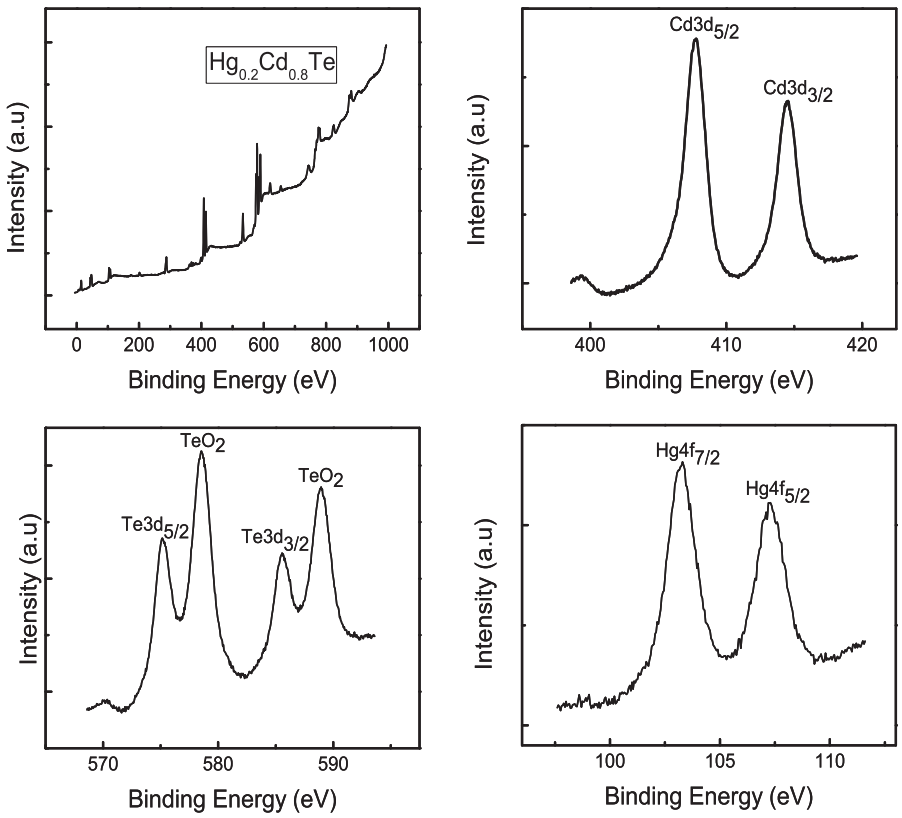

Fig. 2. XPS spectra of $Hg_{1-x}Cd_xTe$ ($x \sim 0.8$).

the dissociative Cd^{2+} and Hg^{2+} ions to form $Hg_{1-x}Cd_xTe$. The reaction to form $Hg_{1-x}Cd_xTe$ can be described as follows [15]:

$$TeO_3^{2-} + N_2H_4{\cdot}H_2O \rightarrow Te + N_2(\uparrow) + 2H_2O + 2OH^- \quad (1)$$

$$2Te + N_2H_4{\cdot}H_2O + 4OH^- \rightarrow 2Te^{2-} + N_2(\uparrow) + 5H_2O \quad (2)$$

$$(1-x)[Hg(en)_2]^{2+} + x[Cd(en)_2]^{2+} + Te^{2-} \rightarrow Hg_{1-x}Cd_xTe(\downarrow) + 2(en) \quad (3)$$

Fig. 1d shows a typical EDS spectra of the sample with $x = 0.8$, which clearly indicates the crystals contain Cd, Hg and Te elements in the atomic percentage of 44.39, 10.0 and 45.59 (with an error bar of 10%) respectively. Fig. 2 shows the typical XPS spectra of $Hg_{1-x}Cd_xTe$ indicating the presence of Hg, Cd and Te in the sample. In the XPS spectra of Te3d there exist two additional peaks of TeO_2. We have done ICP-OES (Inductively Coupled Plasma Optical Emission Spectroscopy) measurement for compositional analysis which shows the presence of Cd and Hg in $Hg_{1-x}Cd_xTe$ with 82% and 18% respectively. Similar observations are made with other compositions as well.

Fig. 3a shows the SEM micrographs of MCT nanorods synthesized in deionized water in the presence of ammonia solution, hydrazine hydrate and surfactant CTAB (Cetyl trimethylammonium bromide). The reactions to form MCT nanorods are same as Eqs. (1) and (2). In this case the metal ion complexes $Cd(NH_3)_4^{2+}$ of Cd and $Hg(NH_3)_4^{2+}$ of Hg are formed by ammonia solution. So the final equation can be written as:

$$xCd(NH_3)_4^{2+} + (1-x)Hg(NH_3)_4^{2+} + Te^{2-} = Hg_{1-x}Cd_xTe(\downarrow) + 4NH_3 \quad (4)$$

The complex reaction to control the nucleation and growth of nanorods is a simple but effective. Our formation mechanisms of MCT nanorods are similar to the mechanism of formation of CdTe nanorods as described by Haibo Gong et al. [16]. In our system, $NH_3{\cdot}H_2O$ was found to be an appropriate and cheap controlling reagent in the formation of MCT nanorods, which helped to form a stable solution by forming $Cd(NH_3)_4^{2+}$, $Hg(NH_3)_4^{2+}$ and avoiding $CdTeO_3$ precipitation before reaction. The uniformity of the solution provides a good environment for the growth of high-quality MCT nanorods. Moreover, the surfactant (CTAB) plays a significant role in the growth of MCT nanorods. When dissolved in water, CTAB can form micelles, which effectively decrease the aggregation of nanoparticles [17]. The mechanism may be that at the initial stage, CTAB adsorbs to the surfaces of newly nucleated MCT nanoparticles and prevents other MCT monomers from freely attaching to the small particles. As a result, at the growth stage some faces are inactive and a special direction is kept as the preferential growth orientation. Therefore, one possible function of CTAB in the present synthetic method is to generate large numbers of rodlike micelles in aqueous solution, which may act as a soft template towards the formation of 1D nanostructures as well as stabilizing the 1D nanostructure [18]. The presence of irregular shape particles along with nanorods in Fig. 3a indicates that CTAB may not satisfactorily perform its role as soft template.

Fig. 3b shows the room temperature FTIR spectra of the MCT prepared in ethylenediamine in the region 0.4–1.5 eV for the composition $x = 0.8$. The spectra show that the band gap of the sample is around 1.1 eV and the absorption onset is at 1 eV. Using Hansen's equation $[E_g = -0.302 + 1.93x + 5.35(10^{-4})T(1-2x) - 0.810x^2 + 0.832x^3]$ the energy band gap, corresponding to $x = 0.80$ at $T = 300$ K is 1.05 eV [19]. Also according to Legros and Triboulet [20] the band gap corresponding to this $x = 0.80$ of $Hg_{1-x}Cd_xTe$ is 1.12 eV indicating that the expected composition of MCT is preserved in the samples. The basic PL behaviour of MCT nano- and micro-crystals

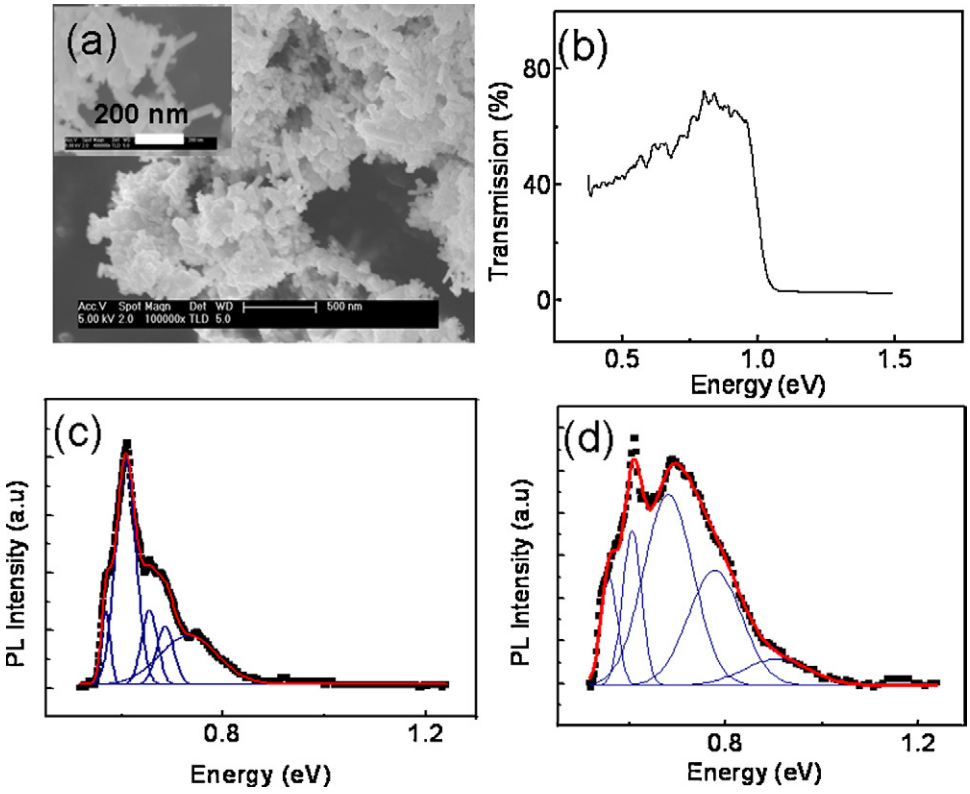

Fig. 3. (A) FESEM image of $Hg_{1-x}Cd_xTe$ ($x \sim 0.8$) nanorods. (B) Room temperature FTIR spectra of $Hg_{1-x}Cd_xTe$ ($x \sim 0.8$) mixed nano- and micro-crystals in NIR region. (C) Room temperature Gaussiana fitted PL spectra of $Hg_{1-x}Cd_xTe$ ($x \sim 0.8$) mixed nano- and micro-crystals. (D) Room temperature Gaussian fitted PL spectra of $Hg_{1-x}Cd_xTe$ ($x \sim 0.8$) nanorods.

at room temperature is demonstrated in Fig. 3c and d. There are five pronounced bands in the region 0.56–0.92 eV at 300 K. As the band gap is found to be 1.1 eV we observe no band edge emission from the sample. The absence of band edge emission indicates that the observed bands are defect related and thus the surface state recombination is the dominant process here. This sample emits in the NIR region which shows that this can be used for photonic application. Though the absorption in the other compositions is quite broad may be due to the large variation in the size of the nano-crystallites, we could not observe luminescence from these samples. This may be attributed to our limitations on the excitation wavelength (514.15 nm). In these samples, it is expected to generate electron–hole pairs close to the surface because of large surface to volume ratio, where the surface recombination plays a dominant role that kills the luminescence efficiency.

4. Conclusions

In summary, using an air-stable and water-soluble Te source, we have synthesized $Hg_{1-x}Cd_xTe$ nanostructures with sizes vary between 20 and 500 nm under two different solvothermal conditions. The experimental results indicated that the morphology of the formed nanocrystallites changed from irregular nanoparticles to nanorods with the use of surfactant, cetyl trimethylammonium bromide (CTAB). A systematic variation in lattice constant is quite consistent with the calculated values using Vegard's law. The PL emission for a sample with $x = 0.8$, in the 0.5–0.9 eV IR region is quite useful for optoelectronic applications. The absence of luminescence in the other compositions is attributed to the limitations on the excitation wavelength. The formation mechanism of MCT nanorods here may also be useful for other semiconductor nanocrystallites analogous to mercury cadmium telluride, such as CdHgSe, CdMnTe etc.

Acknowledgements

One of the authors (J.K.) thanks CSIR, India for providing fellowship to carry out the research at IISc, Bangalore, India. We would like to thank DST National facility for FTIR measurements. We would also like to thank Institute Nanoscience Initiative, IISc for electron microscopy measurements.

References

[1] J. Bajaj, J.M. Arias, M. Zandian, J.G. Pasko, L.J. Kozlowski, R.E. De Wames, W.E. Tennant, J. Electron. Mater. 24 (1995) 1067.
[2] T. Aoki, Y. Chang, G. Badano, J. Zhao, C. Grein, S. Sivananthan, D.J. Smith, J. Cryst. Growth 265 (2004) 224.
[3] B. Tang, F. Yang, Y. Lin, L. Zhuo, J. Ge, L. Cao, Chem. Mater. 19 (2007) 1212.
[4] H. Qian, C. Dong, J. Peng, X. Qiu, Y. Xu, J. Ren, J. Phys. Chem. C 111 (2007) 16852.
[5] J.H. Chu, D.Y. Tang, J. Electron. Mater. 25 (1996) 1176.
[6] P. Capper, Properties of Narrow Gap Cadmium-based Compounds, Institution of Engineering and Technology, London, 1994.
[7] M. Zandian, A.C. Chen, D.D. Edwall, J.G. Pasko, J.M. Arias, Appl. Phys. Lett. 71 (1997) 2815.
[8] A.I. Belogorokhov, A.C. Belov, V.M. Lakeenkov, L.I. Belogorokhova, Appl. Phys. Lett. 72 (1998) 516.
[9] Sadao Adachi, Handbook on Physical Properties of Semiconductors, vol. 3, Kluwer Academic Publishers, Boston, 2004, pp. 360 and 446.
[10] A.R. Denton, N.W. Ashcroft, Phys. Rev. A 43 (1991) 3161.
[11] J.C. Woolley, B. Ray, J. Phys. Chem. Solids 13 (1960) 151.
[12] T. Skauli, T. Colin, J. Cryst. Growth 222 (2001) 719.
[13] Y. Li, Y. Ding, H. Liao, Y. Qian, J. Phys. Chem. Solids 60 (1999) 965.
[14] R.R. Arnepalli, V. Dutta, Mater. Res. Soc. Symp. Proc. 878E (2005).
[15] A.M. Qin, Y.P. Fang, C.Y. Su, Mater. Lett. 61 (2007) 126.
[16] H. Gong, X. Hao, C. Gao, Y. Wu, J. Du, X. Xu, M. Jiang, Nanotechnology 19 (2008) 445603.
[17] M. Chen, L. Gao, J. Am. Ceram. Soc. 88 (2005) 1643.
[18] G.C. Xi, Y.K. Liu, X.Q. Wang, X.Y. Liu, Y.Y. Peng, Y.T. Qian, Cryst. Growth Des. 6 (2006) 2567.
[19] G.L. Hansen, J.L. Schimt, T.N. Casselman, J. Appl. Phys. 53 (1982) 7099.
[20] R. Legros, R. Triboulet, J. Cryst. Growth 72 (1985) 264.